



## Potent and novel 11 $\beta$ -HSD1 inhibitors identified from shape and docking based virtual screening

Guangxin Xia<sup>a,b</sup>, Mengzhu Xue<sup>b</sup>, Lin Liu<sup>a</sup>, Jianxin Yu<sup>a</sup>, Haiyan Liu<sup>a</sup>, Ping Li<sup>a</sup>, Jianfa Wang<sup>a</sup>, Yanlian Li<sup>b</sup>, Bing Xiong<sup>b,\*</sup>, Jingkang Shen<sup>a,b,\*</sup>

<sup>a</sup> Central Research Institute, Shanghai Pharmaceutical Holding Co. Ltd, 898 Ha Lei Road, Zhangjiang Hi-Tech Park, Shanghai 201203, China

<sup>b</sup> State Key Laboratory of Drug Research, Shanghai Institute of Materia Medica, Chinese Academy of Sciences, 555 Zuchongzhi Road, Zhangjiang Hi-Tech Park, Shanghai 201203, China

### ARTICLE INFO

#### Article history:

Received 17 May 2011

Revised 20 July 2011

Accepted 3 August 2011

Available online 8 August 2011

#### Keywords:

11 $\beta$ -HSD1 inhibitor

Virtual screening

Docking

Shape similarity

### ABSTRACT

Several potent and novel 11 $\beta$ -hydroxysteroid dehydrogenase 1 (11 $\beta$ -HSD1) inhibitors were discovered from in silico screening the commercially available Maybridge database. Among them, seven hit compounds showed good affinity, with IC<sub>50</sub> values lower than 100 nM and the best one 3.7 nM. To select the lead for further optimization, computational ADME/T prediction, the CYP3A4 inhibition and 11 $\beta$ -HSD1 over 11 $\beta$ -HSD2 selectivity test were also performed. Taking all of the above factors into consideration, two promising compounds were selected as lead structures for further development. The employed hierarchical virtual screening protocol not only demonstrates its efficiency, but also provides novel and selective compounds for developing 11 $\beta$ -HSD1 inhibitors to protect against metabolic syndrome.

© 2011 Elsevier Ltd. All rights reserved.

The continuous increase in the prevalence of type II diabetes and obesity in these years has become a worldwide health problem. It has been estimated by World Health Organization (WHO) that about 400 million people might be affected by the disease in 2030.<sup>1</sup> There has been a common understanding that 'metabolic syndrome' is associated with type II diabetes and obesity.<sup>2</sup> This syndrome is a collection of many metabolic and cardiovascular abnormalities, such as abdominal obesity, impaired glucose tolerance, dyslipidemia, low levels of high density lipoprotein (HDL), cholesterol, and hypertension.<sup>3–5</sup>

The importance of metabolic syndrome has attracted numerous investigations on genes, proteins, pathways associated with this disease. Among them, glucocorticoid receptor (GR) signaling plays significant role in metabolic regulation.<sup>6–8</sup> Aberrance of this signaling pathway has implicated in the development of several phenotypes of metabolic syndrome. The major activator of GR in human is cortisol, and the adrenal cortex is the major source of circulating cortisol. GR signaling depends not only on the circulating cortisol levels but also on the intracellular production of cortisol through reduction of cortisone, the inactive glucocorticoid. The enzymes catalyzing the conversion between cortisone and cortisol are 11 $\beta$ -hydroxysteroid dehydrogenases (11 $\beta$ -HSDs). Among them, the type 1 of 11 $\beta$ -HSD is mainly responsible for converting cortisone to cortisol. A potential role for 11 $\beta$ -HSD1 inhibitors in

metabolic disease has been established using transgenic mice. Based on these findings, in recent years, the 11 $\beta$ -HSD1 is recognized as a promising target in metabolic disease.<sup>9–11</sup> Many distinct 11 $\beta$ -HSD1 inhibitors have been developed, and some have been entered into clinic trials, such as INCB-13739<sup>12</sup> and AMG-221.<sup>13</sup>

Virtual screening is a complementary tool to high throughput screening to effectively identify novel compounds and have been successfully used in many drug discovery projects.<sup>14–16</sup> Here the shape-based database searching and fast rigid docking was firstly used to narrow down the candidate compounds, and then the relatively time-consuming ligand flexible docking was applied. After that, cherry-picking was conducted to select the compounds based on docked ligand poses to satisfy essential binding features from the previous knowledge of enzyme–inhibitor interactions. The biological evaluation on these purchased compounds identified several novel structures as well as some compounds very similar to known inhibitors. This result reinforce the strength of our virtual screening procedure and the found active compounds will also benefit further drug discovery targeting 11 $\beta$ -HSD1.

Maybridge screening collection is a highly diverse set of lead-like molecules, and has been extensively used to identify various lead compounds for many drug targets. Given its large chemical space coverage,<sup>17</sup> we choose this database for this study. Multiple conformations of the compounds in Maybridge database were generated by OMEGA program to meet the requirement of shape-based searching and rigid docking.<sup>18</sup> The crystal structures of human 11 $\beta$ -HSD1-inhibitor complexes were retrieved from Protein Data Bank (PDB, 2010.10 version), which consists of 15

\* Corresponding authors. Tel.: +86 21 50806600x5407; fax: +86 21 50807088.

E-mail addresses: [bxiong@mail.shncn.ac.cn](mailto:bxiong@mail.shncn.ac.cn) (B. Xiong), [jkshen@mail.shncn.ac.cn](mailto:jkshen@mail.shncn.ac.cn) (J. Shen).

different inhibitors (see [Supplementary data, Table S1](#)). ROCS program was used to conduct the shape-based ligand searching against the Maybridge database by using the ligand conformations presented in these structures as queries.<sup>18</sup> This program is a fast 3D shape comparison application. It is based on the idea that if two molecules are similar, their volume should be overlapped well. During the comparison, the volume of each molecule is represented as smoothed Gaussian function, which then can be used in the minimization procedure to find the global match. In parallel, the fast rigid docking software FRED was adopted to dock the multiple conformations of database compounds into 11 $\beta$ -HSD1 binding site.<sup>18</sup> Similar to ROCS, the FRED program also utilizes the Gaussian function to represent the shape of molecule and protein binding site. This representation can provide docking methods with a more traceable hypersurface to search for likely coordinates of the ligand due to the Gaussian function is a smooth, analytic function. And numerical optimization methods such as Quasi-Newton can be adopted to move the ligand to the correct position in protein binding site. After obtained an ensemble of reasonable poses of ligand by this shape pre-filtering, the traditional scoring functions can be applied to refine the docking conformations. In FRED docking study, the receptor model was prepared from the crystal structure 3H6K with Maestro in Schrodinger software package.<sup>19</sup> This structure is a dimer composed by two chains of 11 $\beta$ -HSD1 and a NADPH as the cofactor. As illustrated in [Figure 1](#), the binding site is largely hydrophobic in nature, and consists of several important residues in enzyme–inhibitor interactions, such as ILE-121, TYR-183, and THR-222 (residue numbered following 3H6K). Default parameters were set in ROCS and FRED software to search the Maybridge database (see the [Supplementary data](#)). In current study, the scoring functions used in FRED consensus scoring comprise shapeGauss, PLP, chemGauss, chemScore and screenScore.

The 1000 top ranking compounds from the shape-based searching and another 1000 compounds from the rigid docking were combined and subjected to the followed ligand-flexible docking by Glide program with default parameters.<sup>20</sup> Though manual

**Table 1**

The statistics of calculated molecular properties of top 200 compounds from Glide docking simulation and purchased 70 compounds

	Mean	SD	Min	Max
Mass	412.2(460.9)	37.8(48.0)	327.5(327.5)	588.3(588.3)
Log <i>p</i>	4.2(3.8)	0.8(3.3)	−13.6(−13.6)	9.26(9.26)
PSA	68.3(82.5)	21.7(30.8)	6.48(6.48)	172.4(172.4)
Arom_ring	2.8(3.8)	0.9(0.9)	1(1)	6(6)
HBA	5.4(5.5)	1.8(2.0)	0(0)	11(11)
HBD	0.5(0.5)	0.6(0.7)	0(0)	4(4)
RB	3.9(5.5)	1.5(1.9)	0(0)	10(10)

inspection, 70 compounds selected from the top 200 molecules were considered as promising inhibitors and purchased for experimental test (the top 200 compounds were listed in [Supplementary data, Table S2](#)).

After Glide docking, the general physicochemical properties of top scored 200 compounds were calculated to analyze the drug-likeness of these compounds. It was found that most of them are within the rule-of-five (RO5) of Lipinski's definition.<sup>21</sup> The properties of final selected 70 compounds were compared with the top 200 subset. As shown in [Table 1](#), the value distribution of the selected 70 compounds is more scattered than ones in the top 200 subset, indicating higher structural diversity. Although RO5 is a general tool to filter the compounds, we mainly use the binding conformation and interaction patterns as the criteria to select the compounds for biological assay. These drug-like information is used later to select better compounds as lead for optimization.

The 11 $\beta$ -HSD1 is a dimer in its active form. Detailed examination of the inhibitor binding site of 11 $\beta$ -HSD1 shows that an alpha helix at the C terminal of another chain is critical for the inhibitor binding. Large groups at the vicinity of this helix may lead to steric clash with the protein. So it is important to include another chain and the cofactor NADPH to set up the binding site model for docking study. The binding modes of docked compounds were subjected to a visualization checking. As illustrated in [Figure 1](#), most of these compounds adopt a pose similar to the inhibitor in crystal

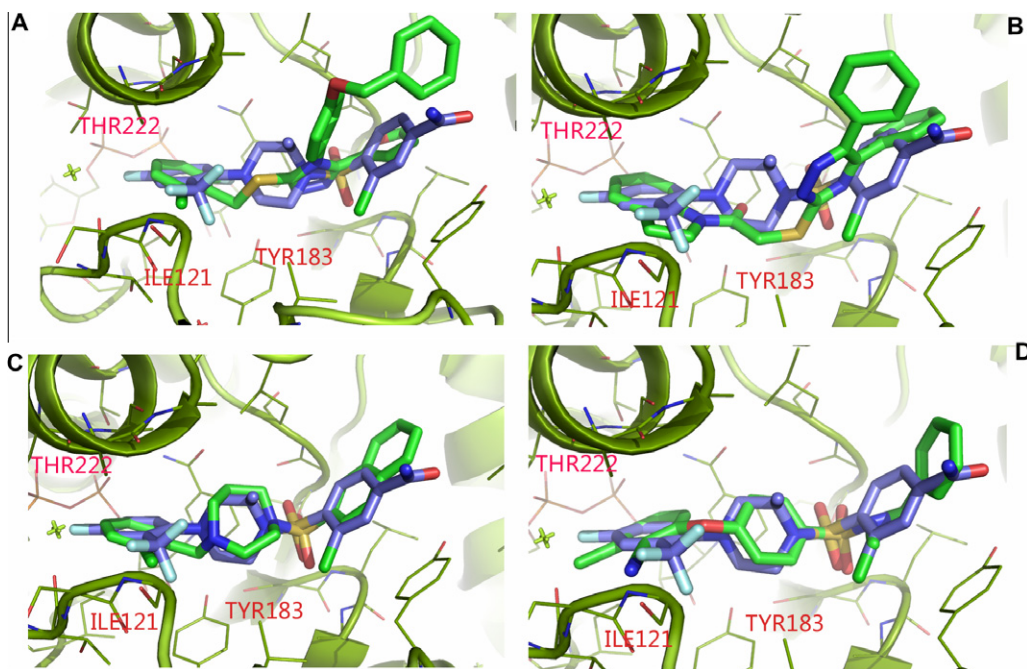


**Figure 1.** Interaction modes of the 11 $\beta$ -HSD1 with inhibitors. The 11 $\beta$ -HSD1 was depicted as ribbon model and colored as pea green and the ligand in crystal structure 3H6K was shown in stick model and colored as purple while the hit structures from in silico screening were colored as green. The conformations of hit structures were from glide docking simulation. Four diverse hit structures were selected for verification. Compound **3** ([Fig. 1A](#)), compound **4** ([Fig. 1B](#)), compound **7** ([Fig. 1C](#)) and compound **8** ([Fig. 1D](#)).

**Table 2**The biological assay result of hit compounds and positive control compound glycyrrhetic acid (**R1**)

Name	Maybridge code	Chemical structure	11 $\beta$ -HSD1 inhibition IC <sub>50</sub> ( $\mu$ M)
Compd 1	SCR00379		0.0288
Compd 2	SEW06024		0.0327
Compd 3	SPB07944		0.0450
Compd 4	HTS12498		0.0581
Compd 5	KM06458		0.0667
Compd 6	DSHS00552		0.1024
Compd 7	AW00745		0.0037
Compd 8	CD07115		0.0413
BVT-14225 <sup>a</sup>	—		0.0284
Glycyrrhetic acid <sup>b</sup>	—		0.0086

<sup>a</sup> BVT-14225 in Ref. 29 has IC<sub>50</sub> 0.052  $\mu$ M.<sup>29</sup><sup>b</sup> Glycyrrhetic acid in Ref. 30 has IC<sub>50</sub> 10 nM.<sup>30</sup>

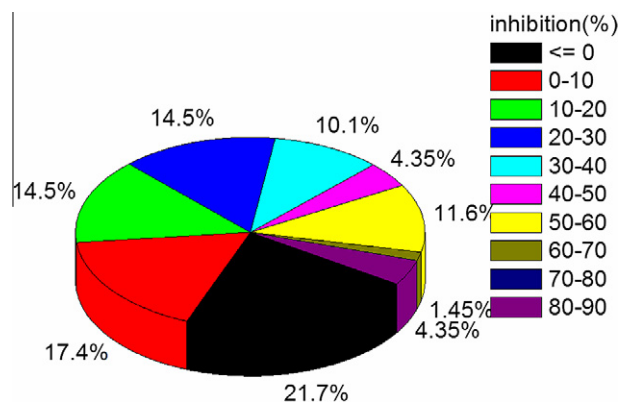


**Figure 2.** Pie plot of the distribution of 11β-HSD1 enzyme assay inhibition ratio at 1 μM.

structure 3H6K, which usually contains two hydrophobic groups at two terminals and a V-shaped connection part in the middle. Many of the middle parts contain a sulfonamide group, and a few others use the ring systems making the right angle to connect the hydrophobic groups. For the terminal hydrophobic groups, most are aromatic rings with various substituents. By analyzing these binding conformations, a new sub-pocket was discovered. Therefore, to test the validity of this finding, we also select a molecule fitting into

three hydrophobic sub-pockets for binding assay (compound **3** in Table 2). Indeed, this compound has a good binding affinity to 11β-HSD1 with IC<sub>50</sub> 45 nM. It is clearly indicated that this new identified sub-pocket could be used to design new series 11β-HSD1 inhibitors with novel scaffolds. Besides for these new chemotype molecules, some similar molecules were identified by ROCS database searching, such as compound **7** and **8** in Table 1, and their docked conformations were illustrated in Figure 1C and D. The oxygen atoms of sulfonamide group contained in each molecule are located at same position compared with the ligand in crystal structure 3H6K. The sulfonamide nitrogen atom of compound **7** is in homopiperazine ring, which is functioned as piperazine in ligand of 3H6K. Differently, the sulfonamide nitrogen atom of compound **8** is on the opposite side and was used to connect the terminal benzene group. Nevertheless, the important hydrogen bonding interactions between sulfonamide group with protein residue Ala-172 are reserved in both compound **7** and **8**, as indicated by their good affinities with 11β-HSD1.

The 70 purchased compounds were tested with a Scintillation proximity assay (SPA) for 11β-HSD1. Inhibition ratio at 1 μM concentration of compounds against human 11β-HSD1 enzymatic activities was determined by using microsomes containing 11β-HSD1 according to previous studies.<sup>22</sup> Briefly, the full-length cDNAs of human or murine 11β-HSD1 were isolated from the cDNA libraries provided by NIH Mammalian Gene Collection and cloned into pcDNA3 expression vector (Invitrogen, Carlsbad, CA, USA) by PCR. HEK-293 cells were transfected with the

**Table 3**

The Pipeline Pilot AMDE/T prediction for the hit compounds and the CYP3A4 experimental inhibition assay at 10 μM

Name	Absorption level <sup>a</sup>	Solubility level <sup>b</sup>	CYP2D6 <sup>c</sup>	PPB level <sup>d</sup>	CYP3A4 inhibition (%) (10 μM)
Compd 1	0	2	0	2	14
Compd 2	0	1	0	1	13
Compd 3	3	1	0	2	73
Compd 4	0	1	1	2	36
Compd 5	0	2	0	2	26
Compd 6	0	2	1	1	82
Compd 7	0	2	0	1	26
Compd 8	0	2	0	2	17

<sup>a</sup> Absorption level 0 means good human intestinal absorption, level 3 means low absorption.

<sup>b</sup> Solubility level 1 means very low solubility at border line of 95% percent of drugs, level 2 indicates low solubility at lower end of 95% percent of drugs.

<sup>c</sup> CYP2D6 0 means non inhibitor, 1 means inhibitor.

<sup>d</sup> PPB level 1 means ≥90% plasma protein binding, and level 2 means ≥95% binding.

HSD1:	35	GKKVIVITGASKGIGREMAHYHLAKMGAAHVVVARSKETLQKVVSCHLELGAASAHYIAGTM
HSD2:	23	TRAVLITGCDSGFGKETAKKLDMSGFTVLATVLELNSP-GATIELR-TCCSPRLRLQLQMDL
HSD1:	95	EDMTFAEQFVAQAGK--LMGGLDMLILNHITNTSLNLFHD--DIHHVRKSMENVNLSYVV
HSD2:	81	TKPGDISRVLEFKAHTTSTGLWGLVNNAGH-NEVVADAELSPVATFRSCMEVNFEGALE
HSD1:	151	LTVAALPMLKQSNQSIIVVSSLAGKVAYPMVAAYSASKFALDGFSSIRKEYSVSRVNV
HSD2:	140	LTGGLLELLRSSRGRIVTVGSPAGDMPYPCLGAYGTSKAAVALIMDTFSCCELL--PWGVK
HSD1:	211	ITLCVLGLIDTETAMKA-----VSGIVHM---QAA
HSD2:	198	VSIIQPGCFKTESVRNVGQWEKRLQLLANLPQELLQAYGKDYIEHLHGQFLHSLRLAMS
HSD1:	238	PKEECALEIIKGGAL--RQEEVYYDSSLWTTLLI
HSD2:	258	DLTPVVDATTDALLAARPRRRYYPG--QGLGLMY

**Figure 3.** Sequence alignment of human 11β-HSD1 and 11β-HSD2. The identity residues are colored yellow, the residues formed NADP binding site are colored blue, and the residues formed ligand binding site are colored red.



pcDNA3-derived expression plasmid and selected by cultivation at the presence of 700  $\mu\text{g}/\text{ml}$  of G418. The microsomal fraction over-expressing 11 $\beta$ -HSD1 was prepared from the HEK-293 cells stable transfected with 11 $\beta$ -HSD1 and used as the enzyme source for SPA. The assay was performed in a 96-well microtiter plate (please see Ref. 22 for details). From the initial inhibition assay, as shown in Figure 2, a total of 14 compounds demonstrate inhibition more than 50% at concentration 1  $\mu\text{M}$ . Eight compounds bear different scaffolds with high inhibition ratio were selected to further binding affinity assay to get the  $\text{IC}_{50}$  values. As shown in Table 2, all 8 compounds have the  $\text{IC}_{50}$  value better or close to 100 nM. Compound 7 has an  $\text{IC}_{50}$  value of 3.7 nM, which is almost as good as the well optimized molecules.

Since all the compounds show good activities to 11 $\beta$ -HSD1, it is a challenge to select compounds for further drug development. By utilizing the ADME/T models implemented in Pipeline Pilot,<sup>23</sup> we calculated some ADME/T related properties of these active compounds. As listed in Table 3, the predicted human intestinal absorption of compound 3 is low, while other compounds are shown good sign in absorption prediction. Compound 4 and 6 may cause CYP2D6 inhibition as predicted from the model. To validate the prediction, we further assessed the compounds with CYP3A4 inhibition studies.<sup>24</sup> Compound 6 shows the highest inhibition ratio of 82% at 10  $\mu\text{M}$  concentration. The compound 4 shows 36% inhibition, slightly higher than other compounds except compound 3. The correlation between computational prediction and real inhibition assay increase our confidence to select the lead compounds based on the ADME/T prediction information.

At the same time, the intelligent patent searching was performed and found that the core structures of SCR00379 (compound 1),<sup>25</sup> SEW06024 (compound 2),<sup>26</sup> and AW00745 (compound 7),<sup>27</sup> 4-phenyl-1,2,3,6-tetrahydropyridine, 1-(pyridin-2-yl) piperazine and diazepane derivatives have been reported as 11 $\beta$ -HSD1 inhibitors and protected by patents. KM06458 (compound 5) was not considered as promising hit since it was reported as a tyrosine kinase inhibitor,<sup>28</sup> which we suspect it may cause cell toxicity. Taking all these information into account, we picked the compounds 4 and 8 are promising leads for further optimization.

In addition, the compounds 4 and 8 were further checked for selectivity over human 11 $\beta$ -HSD2. The results of the enzyme assay show that compound 4 has an  $\text{IC}_{50}$  value of 8.9  $\mu\text{M}$  against human 11 $\beta$ -HSD2, with a selectivity ratio about 200-fold. While for compound 8, even at 100  $\mu\text{M}$ , the inhibition is less than 50%. So the selectivity ratio of compound 8 is at least 2420-fold, which is excellent for a lead compound. To further investigate the ligand selectivity mechanisms between 11 $\beta$ -HSD1 and 11 $\beta$ -HSD2, the residues lining the binding site of 11 $\beta$ -HSDs were compared. As shown in Figure 3, it can be found that the binding site residues were very different for the two enzymes. For the residues 215–222 of 11 $\beta$ -HSD1, which constitute the inner hydrophobic sub-pocket, the 11 $\beta$ -HSD1 generally has larger side chains as compared with residues located at same position in 11 $\beta$ -HSD2. This may account for the high 11 $\beta$ -HSD1 selectivity due to favorable interactions between the inhibitors with these residues. While in 11 $\beta$ -HSD2, the inhibitors may not fully occupy the inner sub-pocket, and as such only show moderate inhibitions. Nevertheless, this important information will assist medicinal chemists to explore the structure–activity-relationship in depth.

To further explore more public available compounds similar to the hit structures in present work, we searched the PubChem database with our eight hit molecules in Table 1 at similarity cutoff value 0.9, and resulted 592 molecules in total. By analyzing the result (see the Supplementary data) from PubChem database, it was found that two compounds (CID: 44237023 and 24901355) were tested in a 11 $\beta$ -HSD1 inhibition assay with  $\text{IC}_{50}$  of 13 and 11 nM, respectively. These two compounds are both very similar to hit

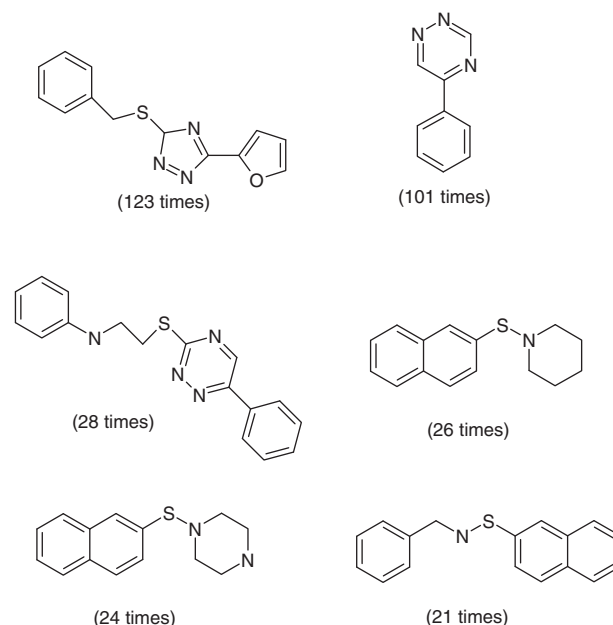


**Figure 4.** The common scaffolds identified from analyzing the result of PubChem similarity searching with our hit compounds. The cutoff value of similarity searching is 0.9, and the number in parentheses indicates how many times this scaffold occurs in the result dataset of similarity searching.

compound 2, and contains the sulfonylpiperazine scaffold. Detailedly investigating the result from the PubChem similarity search, it was clearly shown that the terminal hydrophobic groups are mostly variable and usually consist of aromatic rings with mono-substituted or poly-substituted halogens. The scaffold patterns of the resulting molecules were also analyzed with the in-house program,<sup>31</sup> and the common scaffolds are illustrated in Figure 4. As expected, the scaffolds resemble the hit compounds listed in Table 1. In addition, the analysis simultaneously provides the occurrence frequency information of each scaffold. It was shown that the triazole scaffold is more abundant in PubChem dataset, and followed by triazine scaffold. These are all novel scaffolds in 11 $\beta$ -HSD1 inhibitors, and will empower researchers to explore the possibilities to develop new chemotypes of 11 $\beta$ -HSD1 inhibitors, either by directly purchasing the similar commercially available compounds from vendors, or by synthesizing the analogs in the laboratory.

In conclusion, we have identified several high potent and novel inhibitors of 11 $\beta$ -HSD1 by using virtual screening methods. Through the biological testing, it was demonstrated that the procedure combining shape-based ligand searching with routine docking simulation against the commercial available compounds is efficient in finding novel active molecules. To further assess these hit compounds for optimization, *in silico* ADME/T properties of these hits were calculated to check the druggability. Besides this, the CYP3A4 inhibition assay was adopted to verify the druggability prediction results. Finally, two compounds were selected as leads for further optimization.

## Acknowledgments

We are indebted to Professor Ying Leng, SIMM for 11 $\beta$ -HSD1 assay, and Professor Mingyue Zheng for critically reading the manuscript. We are grateful for the financial support from Shanghai Postdoctoral Sustentation Fund (Grant No. 07R214213 to G.X.) and State Key Program of Basic Research of China (Grant 009CB918502 to B.X.).

## Supplementary data

Supplementary data associated with this article can be found, in the online version, at doi:10.1016/j.bmcl.2011.08.019.

## References and notes

1. <http://www.who.int/diabetes/en/>.
2. Kahn, R.; Buse, J.; Ferrannini, E.; Stern, M. *Diabetologia* **2005**, *48*, 1684.
3. Bonora, E. *Ann. Med.* **2006**, *38*, 64.
4. Hu, G.; Qiao, Q.; Tuomilehto, J. *Curr. Diab. Rev.* **2005**, *1*, 137.
5. Matfin, G. *Curr. Diab. Rep.* **2008**, *8*, 31.
6. Rose, A. J.; Vegiopoulos, A.; Herzig, S. *J. Steroid Biochem. Mol. Biol.* **2010**, *12*, 210.
7. Tomlinson, J. W.; Stewart, P. M. *Best Pract. Res. Clin. Endocrinol. Metab.* **2007**, *21*, 607.
8. Rosmond, R. *Obes. Res.* **2002**, *10*, 1078–1086.
9. Saiah, E. *Curr. Med. Chem.* **2008**, *15*, 642–649.
10. Wamil, M.; Seckl, J. R. *Drug Discovery Today* **2007**, *12*, 504.
11. Hale, C.; Wang, M. *Mini. Rev. Med. Chem.* **2008**, *8*, 702.
12. Tiwari, A. *IDrugs* **2010**, *13*, 266.
13. Véniant, M. M.; Hale, C.; Hungate, R. W.; Gahm, K.; Emery, M. G.; Jona, J.; Joseph, S.; Adams, J.; Hague, A.; Moniz, G.; Zhang, J.; Bartberger, M. D.; Li, V.; Syed, R.; Jordan, S.; Komorowski, R.; Chen, M. M.; Cupples, R.; Kim, K. W.; St Jean Jr, D. J.; Johansson, L.; Henriksson, M. A.; Williams, M.; Vallgård, J.; Fotsch, C.; Wang, M. *J. Med. Chem.* **2010**, *53*, 4481.
14. Klebe, G. *Drug Discovery Today* **2006**, *11*, 580.
15. Sousa, S. F.; Cerqueira, N. M.; Fernandes, P. A.; Ramos, M. J. *Comb. Chem. High Throughput Screen.* **2010**, *13*, 442.
16. Villoutreix, B. O.; Eudes, R.; Miteva, M. A. *Comb. Chem. High Throughput Screen.* **2009**, *12*, 1000.
17. Krier, M.; Bret, G.; Rognan, D. *Chem. Inf. Model.* **2006**, *46*, 512.
18. OMEGA, ROCS and FRED program <http://www.eyesopen.com>.
19. Wan, Z. K.; Chenail, E.; Xiang, J.; Li, H. Q.; Ipek, M.; Bard, J.; Svenson, K.; Mansour, T. S.; Xu, X.; Tian, X.; Suri, V.; Hahm, S.; Xing, Y.; Johnson, C. E.; Li, X.; Qadri, A.; Panza, D.; Perreault, M.; Tobin, J. F.; Saiah, E. *J. Med. Chem.* **2009**, *52*, 5449.
20. <http://www.schrodinger.com>.
21. Lipinski, C. A.; Lombardo, F.; Dominy, B. W.; Feeney, P. J. *Adv. Drug Deliv. Rev.* **2001**, *46*, 3.
22. *Scintillation proximity assay (SPA) for 11 $\beta$ -HSDs*: Different concentrations of compound were added, followed by addition of 80  $\mu$ L of 50 mM HEPES buffer, pH 7.4 containing 25 nM cortisone[1,2-(n)<sup>3</sup>H] (Amersham, Buckinghamshire, UK) and 1.25 mM NADPH (for 11 $\beta$ -HSD1 assay) or 12.5 nM cortisol[1,2,6,7-(n)<sup>3</sup>H] (Amersham, Buckinghamshire, UK) and 0.625 mM NAD (for 11 $\beta$ -HSD2 assay). Reactions were initiated by the addition of 11 $\beta$ -HSD1, enzyme preparation as microsomal fractions from HEK293 cells in a final concentration of 80  $\mu$ g/mL for 11 $\beta$ -HSD1. Following 60 min incubation at 37 °C, the reaction was stopped by addition of 35  $\mu$ L of 10 mg/mL protein A-coated SPA beads (GE, Piscataway, NJ, USA) suspended in Superblock Blocking Buffer (Pierce, Rockford, IL) with 3  $\mu$ g/mL of murine monoclonal cortisol antibody (East Coast Biologics, North Berwick, Maine, USA) and 314 M glycyrrhethinic acid (Sigma–Aldrich, St. Louis, MO). The plates were incubated under plastic film on an orbital shaker for 120 min at room temperature before counting. The amount of [<sup>3</sup>H]cortisol generated in 11 $\beta$ -HSD1 enzyme reaction was captured by the beads and determined in a microplate liquid scintillation counter. Percent inhibition was calculated relative to a non-inhibited control. Data were obtained from at least three independent experiments. IC<sub>50</sub> values were calculated by using Prism Version 4 (GraphPad Software, San Diego, CA).
23. <http://www.accelrys.com>.
24. *CYP3A4 assay*: The incubation system was 100  $\mu$ L of human liver microsomes (final concentration 0.2 mg/mL) and contained 1 mM NADPH and 10  $\mu$ M test compound or positive inhibitors cocktail (Ketoconazole 10  $\mu$ M, Quinidine 10  $\mu$ M, Sulfaphenazole 100  $\mu$ M) or negative control PBS. After incubation for 20 min, 100  $\mu$ L of acetonitrile was added to stop the reaction. The supernatant was transferred to perform analysis after centrifugation at 10,000 $\times$ g and 4 °C for 10 min. The assays were performed using LC/MS/MS. Inhibition percentage was calculated from the comparison of the production of metabolite to the negative control.
25. Aertgeerts, K.; Brennan, N. K.; Cao, S. X.; Chang, E.; Kiryanov, A. A.; Liu, Y. WO2006105127, 2006; *Chem. Abstr.* **2006**, *145*, 419173.
26. Xiang, J. S.; Saiah, E.; Tam, S. Y.; Mckew, J. C.; Chen, L.; Ipek, M.; Lee, K.; Li, H.; Li, J.; Li, W.; Mansour, T. S.; Suri, V.; Vargas, R.; Wu, Y.; Wan, Z.; Lee, J.; Binnun, E.; Wilson, D. P. WO2007092435, 2007; *Chem. Abstr.* **2007**, *147*, 277637.
27. Caulkett, P. W. R.; Mccoull, W.; Packer, M.; Whittamore, P. R. O. WO2007135427, 2007; *Chem. Abstr.* **2008**, *148*, 33765.
28. Tang, P. C.; Sun, L.; Nematalla, A. S.; McMahon, G. WO9640629, 1996; *Chem. Abstr.* **1996**, *126*, 139910.
29. Barf, T.; Vallgård, J.; Emond, R.; Häggström, C.; Kurz, G.; Nygren, A.; Larwood, V.; Mosialou, E.; Axelsson, K.; Olsson, R.; Engblom, L.; Edling, N.; Rönquist-Nii, Y.; Ohman, B.; Alberts, P.; Abrahmsén, L. *J. Med. Chem.* **2002**, *45*, 3813.
30. Zhang, X.; Zhou, Z.; Yang, H.; Chen, J.; Feng, Y.; Du, L.; Leng, Y.; Shen, J. *Bioorg. Med. Chem. Lett.* **2009**, *19*, 4455.
31. Yan, B. B.; Xue, M. Z.; Xiong, B.; Liu, K.; Hu, D. Y.; Shen, J. K. *Acta Pharmacol. Sin.* **2009**, *30*, 251.